Direct Observation of Solidification and Phase Transformation in Pure Titanium

KOMIZO Yu-ichi*, TERASAKI Hidenori*, SAIKI Keita and IKEDA Masahiko*****

Abstract

Unidirectional-solidification and phase transformation in the weld metal of commercial pure-titanium in Gas Tungsten Arc welding was observed by using Time-Resolved X-Ray Diffraction (TRXRD) system with two-dimensional pixel detector. An undulator beam was used as a probe. A larger area of a cone of half apex angle 2θ made by diffracted beam could be detected in the time-resolution of 0.05 seconds, in unidirectional solidification and subsequent phase transformation process of pure-titanium weld metal. The constrained growth of weld metal in solidification processes and rapid change of phase ratio in β-α transformations were clearly shown.

KEY WORDS: (welding), (solidification), (β-α transformation), (TRXRD), (undulator beam), (titanium)

1. Introduction

Understanding and controlling solidification and phase transformation processes of weld-metal is essential for forming microstructures with superior mechanical properties. For example, solidification mode controls the segregation phenomena [1)] and dispersed position of non-metallic inclusions [2)]. Then it significantly affects subsequent phase transformation phenomena and formed microstructures.

Recent evolution of analysis techniques allows the solidification and phase transformation to be analyzed in-situ, in direct and reciprocal lattice space. Trivedi et al selected succinoritrile-1.2 wt% acetone as an analog for an alloy metal and the solidification process was characterized in-situ [3)]. Their characterizations have clearly shown a grain selection process during welding, with several other phenomena including epitaxial growth and porosity formation. Since the late 1990s, Spatially and Time-Resolved X-Ray Diffraction (SRXRD, TRXRD) experiments using synchrotron radiation have been applied to observation of heat affected zone [4-6)] and weld metal [7-10)] in unidirectional welds, and in spot welding [11)]. In our previous work [8)], the phase evolution of the weld metal of hypereutectoid steel in Gas Tungsten Arc (GTA) welding was observed in-situ by using a one-dimensional imaging plate camera. The one-dimensional camera could detect a part of a cone of half apex angle 2θ made by the diffracted beam. Furthermore the imaging plate should be replaced in the experiment during thermal cycles of the weld. Thus, the detailed nature for solidification and phase transformations in weld metal could not be presented.

In the present work, The TRXRD system consisting of a two-dimensional pixel detector [12)] and undulator-beam probe was applied in order to observe unidirectional-solidification and phase transformation in the weld metal of commercial pure-titanium in GTA welding. The novel-wide detector and ultra-bright probe allowed phase evolution during GTA welding to be observed in the time-resolution of 0.05 seconds.

The well-aligned dendrites in the solidification stage and subsequent rapid changes of phase ratio in β-α transformation were clearly shown.

2. Experimental methods

2.1 Materials and welding

GTA welding was conducted on plate (150 mm×50 mm×12mm) of commercial pure-titanium (Ti-0.019%Fe-0.047%O). The sample was set on a

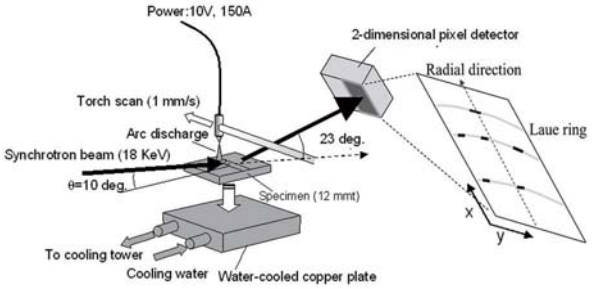

Fig.1 Schematic illustration of time-resolved X-ray diffraction experiment system set in undulator beam-line (BL46XU) of SPring 8 (JASRI).

†Received on July 10, 2009
*Professor
**Graduate Student
***Professor, Kansai University

Transactions of JWRI is published by Joining and Welding Research Institute, Osaka University, Ibaraki, Osaka 567-0047, Japan

water-cooled copper anode. The shielding gas was pure argon and the flow-rate was 15 l/min. The arc current was

Table 1 Calculated 2q of b-Ti (B. C. C.) and a-Ti (H. C. P.) peaks that can appear from 14.85 to 30.95 degrees (angles in the camera window used).

Phase	2θ	hkl	Intensity (powder)
α-Titanium	15.50	100	241.5
	16.94	002	251.0
	17.68	101	1000.0
	23.02	102	149.2
	27.00	110	176.8
	30.00	103	184.8
β-Titanium	17.08	110	1000.0
	24.24	200	172.0
	29.82	211	342.5

150 A and the arc length was kept at the length of 2 mm (arc voltage of 10 V). Fixing the plasma torch on the stepping motor stage, the welding speed was controlled at a constant speed of 1 mm/sec. The welding system consisting of plasma torch, stepping motor stage, sample and water-cooled copper anode was set on a multi-axis diffractometer in the beam line of a synchrotron radiation source (SPring8).

2.2 Time-Resolved X-ray Diffraction (TRXRD) system

The schematic illustration of the TRXRD experimental system is shown in **Fig. 1.** The TRXRD experiments were performed in undulator beam line (BL46XU) in the third generation synchrotron radiation source, SPring8 (JASRI). The ultra-bright, directional, quasi-monochromatic natures of the beam [13] were suitable as the probe for our purpose, i.e., time-resolved observation of solidification and phase transformation process during GTA welding of weld metal. The undulator beam was monochromatized with Si(111) double-crystals to an energy of 18 keV. The sample and torch were tilted at 10° (θ=10°) to the incident beam. The beam slit size was 100×500 μm. Thus, the irradiated area resulted in a normal of 2.88 mm and parallel of 0.1 mm to the welding direction. The irradiated area was fixed on the sample and the arc plasma traversed this area. The formed width of weld-bead was 10 mm. The diffraction patterns under heating, melting and cooling cycle of GTA welding were dynamically recorded with a two-dimensional pixel detector [12]. The time-resolution was 0.05 seconds in which a readout-time was only 8 ms. The dynamic range of the camera was 20 bit. The detector was fixed at the elevation angle of 23° (fixed 2 θ) and the camera length that resulted was 295.5619 mm. The low elevation angle reduced the error in width of diffraction peaks arising from the footprint of the X-ray beam [6]. The error amounted to four pixels in a scattering angle of 23°. The detector area of camera consisted of 487×195 pixels and the unit pixel size was 172 μm. These conditions described above determined the scattering angle (2θ) range of 14.85-30.95°. In this scattering range, a cone of half apex angle 2θ made by diffracted beam was recorded as showed in **Fig. 1**. The calculated scattering angles for β-titanium (B.C.C) and α-titanium (H. C. P.) and the intensity (powder) within this camera window are shown in **Table 1**.

2.3 High-temperature Laser Scanning Confocal Microscopy (HLSCM) system

The High-Temperature Laser Scanning Confocal Microscopy (HLSCM) system (**Fig. 2**) was used for direct observation of the microstructure development along the thermal cycles. The details of the experimental setup are described elsewhere [10]. The prepared samples were machined into a size of 5.3 mmφ and <1.0 mm height and the observed plane was mirror polished. The optical system of HLSCM allows the focused point to be detected in a CCD detector. The focused point is scanned by an acoustic optical device and images are made at a 30-frame rate. This allows microstructure development along a thermal cycle to be observed in-situ at high temperature and high time-resolution. In the present work,

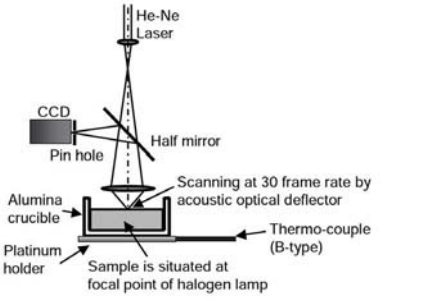

Fig.2 Schematic illustration for sample in infrared furnace and optical system in HLSCM.

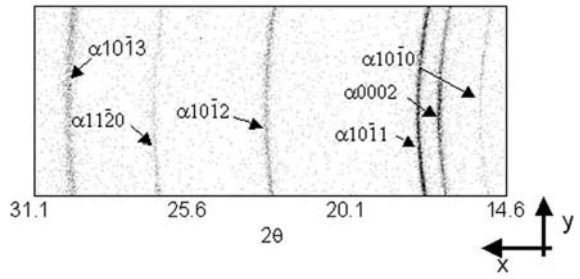

Fig. 3 Diffraction pattern for as-received pure-titanium plate before welding, in room temperature.

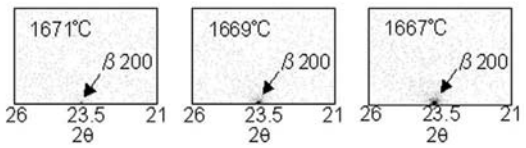

Fig. 4 Spot diffraction patterns for primary b-phase.

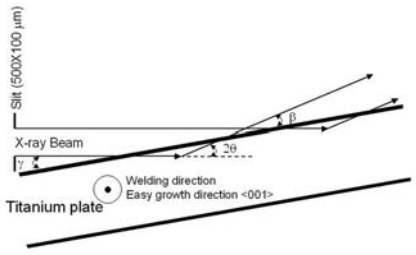

Fig. 5 Schematic representation of scattering geometry used.

the thermal cycle: heating from room temperature to 1543℃ in 55 seconds and then cooling to 400 ℃ in 39 seconds (5 seconds from 900 to 700 ℃), was applied in order to assess the β-α phase transformation.

3. Results and Discussion

Figure 3 shows the acquired diffraction pattern for base metal before welding. The x-y axis corresponds to the one in **Fig. 1**. Each hkl cone was recorded in the camera. The random orientation of grains in the base metal caused the diffraction to be a ring pattern. After showing the halo pattern corresponding to the liquid phase, well-aligned dendrite microstructure in unidirectional solidification caused diffractions to be spot pattern as shown next. **Figure 4** shows the spot diffraction patterns for β-titanium phase in the unidirectional solidification process (enlarging in the angle of 21-26 degree). It was clear that the two-dimensional camera allowed the fringe spot pattern to be detected. Only β200 reflection was detected although there were three planes in the measuring angle of the camera, as shown in **Table 1**. Furthermore, the β200 diffraction pattern did not

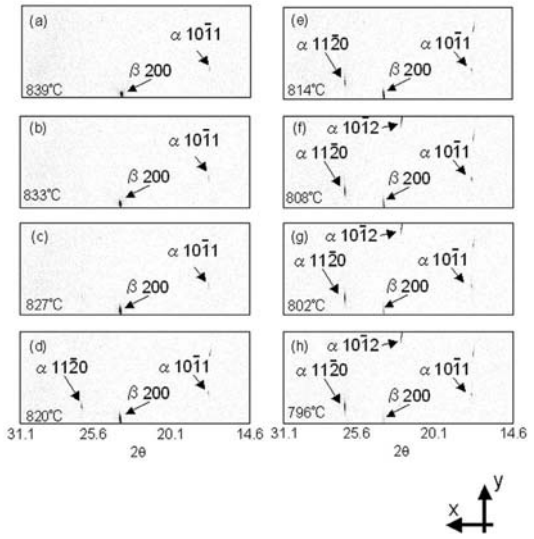

Fig.6 Diffraction patterns for b-a transformation of pure-titanium weld in 0.1 second interval.

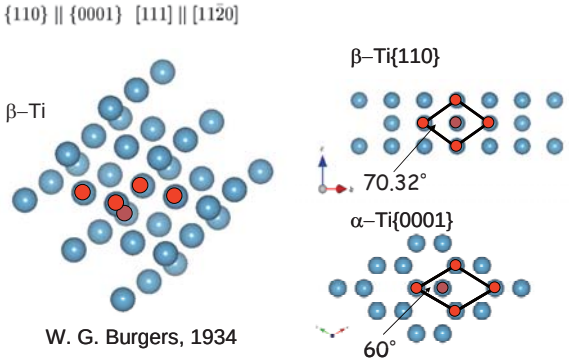

Fig. 7 β－α transformation in pure titanium

distribute along the y-direction of the camera. The temperatures were based on calculated results by a using quasi-steady state model [15], throughout the present work. A primary phase originated at partially-melt base metal and it nucleated in epitaxial from[3], with a little undercooling. Thus, the temperature in **Fig. 4** (1671 ℃) was almost same as the equilibrium temperature of 1668 ℃. The scattering geometry for the present experiments is shown in **Fig. 5.** The penetration depth of X-rays can be estimated using the geometry. The γ and β in **Fig. 5** is an angle of the incident and the scattering X-ray beam vector to the surface line of the titanium plate, respectively. The X-ray absorption coefficients μ of titanium element was 89.109 cm^{-1} using a titanium density just under the melting point [16] and the mass absorption coefficient was 17.97 keV [17]. The penetration depth of X-rays, t, can be estimated as follows:

$$\int_0^t \frac{I_0}{\sin\gamma} e^{-\mu x(1/\sin\gamma+1/\sin\beta)}dx = G\cdot\int_0^\infty \frac{I_0}{\sin\gamma} e^{-\mu x(1/\sin\gamma+1/\sin\beta)}dx \quad \textbf{(1)}$$

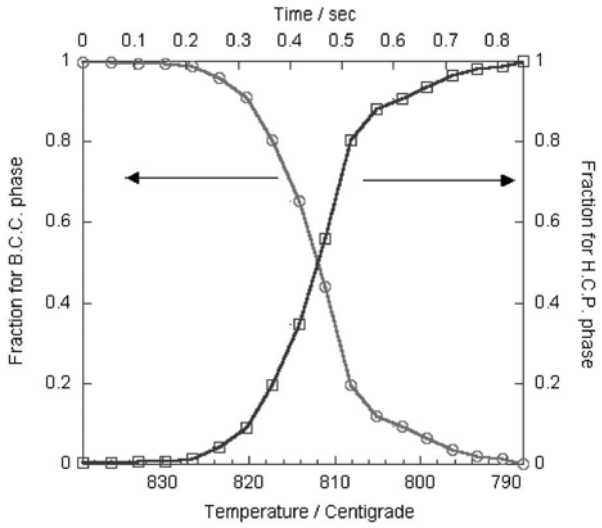

Fig.8 Semi-evaluated change of phase ratio between B. C. C. and H. C. P. phase.

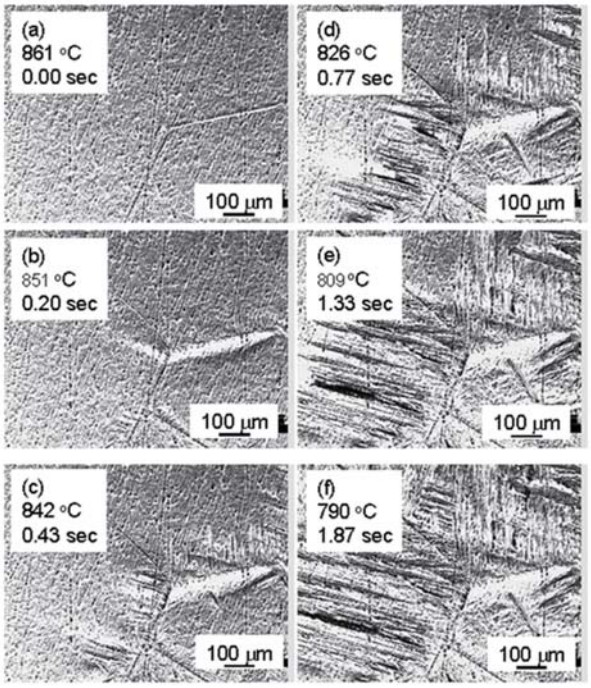

Fig.9 In-situ observation of morphological development in β - α phase transformation in cooling rate of 37.75℃/s.

where G is scattering intensity ratio to total scattering intensity within t penetration depth. When G=0.99, the penetration depth can be estimated as 50.646μm. Thus, it could be calculated that dendrites in 0.0146 mm^3 were observed in **Fig. 4**. Within this volume, many dendrites cecurred but only β200 reflection kept satisfying the Bragg law during the cooling thermal cycle of welding. Taking into account that the X-ray beam was introduced and the camera was fixed as shown in Fig. 1, the result showed that dendrites did not rotate around growing axes (easy growth direction <001>) during the growing process. If they rotated, the reflection that satisfy the Bragg law would change during the cooling thermal cycle of welding. Furthermore it is clear that growing dendrites were highly oriented around the primary X-ray beam. If they are miss-oriented around the primary X-ray beam, the diffraction pattern distributed along the y-direction of the camera. However the diffraction pattern showed a spot-shape as shown in **Fig. 4**. Those features made for an orientation relationship between the planes to be semi-evaluated in subsequent phase transformation. In this case, the habit plane related to β200 could be evaluated.

Figure 6 shows diffraction patterns in β-α phase transformations in the interval of 0.1 seconds. At 839℃, a diffraction pattern for α was detected. The equilibrium β-α transition is 882 ℃ and the undercoolings resulted in 43℃. As temperature decreased, the photon number of the $\alpha 10\bar{1}1$ diffraction pattern increased and other reflections of $\alpha 11\bar{2}0$ and $\alpha 10\bar{1}2$ were detected. We observed unidirectional solidification and the β200 plane was detected because it satisfied the Bragg law in the current experimental setup. It did not mean all dendrites in the observation volume had the same crystal orientation. However, it could be concluded that the dendrite did not rotate along a growing axis. Thus the orientation relationship between β and α planes can be semi-evaluated. Between those three α-planes ($\alpha 10\bar{1}1$, $\alpha 11\bar{2}0$ and $\alpha 10\bar{1}2$), the $\alpha 10\bar{1}2$ showed the strongest intensity of diffraction at 788 ℃. It corresponded to the fact that the $\alpha 10\bar{1}2$ plane and β200 plane makes a habit plane in the Burgers Orientation Relationship [18] as shown in **Fig.7**. The photon number of β 200 reflection decreased due to a lowering phase ratio in the cooling cycle. At 788 ℃, only diffraction patterns for α-phase were observed. A semi-quantitative evaluation of phase ratio change between β and α phase was derived comparing the integration of photon numbers detected in the camera for each phase. The result is summarized in **Fig. 8**. Within 0.85 seconds, whole of B. C. C. phase transformed to H. C. P. phase.

Figure 9 shows the microstructure development for pure Ti during rapid cooling. The phase transformation started at 861 ℃ as shown in **Fig. 9 (a)** and the nucleation site resulted in grain boundary of β-phase. The start time of the phase transformation is set to zero as shown in **Fig. 9 (a)**. Well-aligned lath plate was developing as clearly shown in **Fig. 9 (c)-(f)** and completed the phase transformation. The developing speed resulted in about 337 μm per second, that is slower than that of displacive phase transformation. When slower cooling rate (59 seconds from 900 to 700 ℃) was applied to the sample, the phase transformation started at 878 ℃ and the developing speed of the plate resulted in 122 μm per second. Those cooling rate dependence of β-transus and growth rate were characteristic of reconstructive phase transformation.

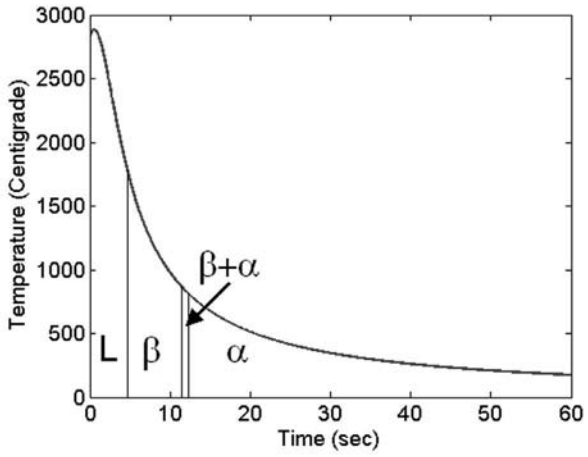

Fig. 10 Phase transformation in cooling cycle of weld are summarized with cooling time and temperature (L, b and a denotes liquid, b-titanium and a-titanium, respectively).

Finally the summarized results of phase evolution in the

TRXRD experiments with time and temperature are shown in **Fig. 10.** In future work, a two-dimensional camera with larger area will be used. This will make it possible to evaluate an orientation relationship at phase transformations with the larger area of Ewald sphere.

4. Conclusions

(1)Unidirectional solidification and phase transformations for pure-titanium were observed in-situ in reciprocal lattice space. An ultra-bright undulator beam and novel-two dimensional pixel camera made this possible.

(2)Dendrites did not rotate along easy growth direction and were highly oriented around primary X-ray beams under unidirectional solidification in GTA welding. This is due to the constrained growth made by the GTA plasma source and the welded material. Thus the diffraction pattern became a spot and the same plane kept satisfying the Bragg law during the solidification process.

(3)The semi-quantitative evaluation of phase ratio during β-α transformation was shown by using the photon number of the diffracted beam.

Acknowledgments

This work was performed at Spring-8 BL46Xu and the authors appreciate for the staffs of JASRI. The synchrotron adiation experiments were performed at the Spring-8 with the approval of the Japan Synchrotron Radiation Research Institute (JASRI) (ProposalNo.2006A0257-NI-np-TU, 007B0363-NI-np).

REFERENCES

1) A. O. Kluken, O. Grong and Grorvik, Metall. Mater. Trans. A, 21A (1990), pp. 2047-58.
2) A. A. B. Sugden and H. K. D. H. Bhadeshia, Metall. Mater. Trans. A, 19A (1988), pp. 669-674.
3) R. Trivedi, M. A. Eshlman, J. M. Vitek, S. S. Babu, T. Hong, T. Debroy: J. Appl. Phys., 93, (2003), pp. 4885-95.
4) J. W. Elmer, J. Wong, M. Froba, P. A. Waideand E. M. Larson, Metall. Trans. A, 27A, (1996), pp. 775-783.
5) J. Wong, M. Froba, J. W. Elmer and P. A. Waide, J. Mat. Sci., 32, (1997), pp. 1493-1500.
6) T. Ressler, J. Wong and J. W. Elmer: J. Phys. Chem. B, 102, (1998), pp. 10724-735.
7) Y. Komizo, H. Terasaki, M. Yonemura and T. Osuki, Transactions of JWRI, 34, (2005), pp. 51-55.
8) H. Terasaki, Y. Komizo, M. Yonemura and T. Osuki, Metall. Mater. Trans. A, 37A, (2006), pp. 1261-66.
9) M. Yonemura, T. Osuki, H. Terasaki, Y. Komizo, M. Sato and A. Kitano, Materials Transactions, 47-2(2006), pp.310-316.
10)Y.Komizo, H.Terasaki, M.Yonemura and T.Osuki, Welding in the World, 52-5/6(2008), pp.56-63
11) S. S. Babu, J. W. Elmer, J. M. Vitek and S. A. David, Acta Mater., 50, (2002), pp. 4763-4781.
12) E. F. Eikenberry, Ch. Bronnimann, G. Hulsen, H. Toyokawa, R. Horisberger, B. Schmitt, C. Schulze-Briese and T. Tomizaki: Nucl. Instr. And Meth. A, 501, (2004), pp. 260-266.
13) H. Kitamura, S. Tamamushi, T. Yamakawa, S. Sato, Y. Miyahara, G. Isoyama, H. Nishimura, A. Mikuni, S. Asaoka, S. Mitani, H. Maezawa, Y. Suzuki, H. Kanamori and T. Sasaki, Jpn. J. Appl. Phys., 21, (1982), pp. 1728-1731.
14) H. Terasaki and Y. Komizo, Sci. Technolo. Weld. Joining., 11-5(2006), pp.561-566.
15) J. C. Ion, K. E. Eastering and M. F. Ashby: Acta metal., 32, (1984), , pp. 1949-1962.
16) S. R. Seagle, P. A. Russo: Principles of alloying Titanium (A lesson from Titanium and its alloys), ASM International, Materials Park, Ohio, 1994, pp. 5.
17) S. Sasaki, KEK Report, 90, (1990), pp. 1-143.
18) Y. Ohmori, H. Natsui and K. Nakai: Mater. Trans., 42, (1998), pp. 49-56.